Hindered Diffusion of Polystyrene in Controlled Pore Glasses

Yihong Guo,† Kenneth H. Langley,*,‡ and Frank E. Karasz†

Department of Polymer Science and Engineering and Department of Physics and Astronomy, University of Massachusetts, Amherst, Massachusetts 01003.
Received June 8, 1989; Revised Manuscript Received October 10, 1989

ABSTRACT: The diffusion of a flexible polymer (polystyrene) in fluid-filled pores of silica controlled pore glasses has been studied by using dynamic light scattering. Each measurement was carried out inside a single porous glass fragment that was immersed in a solution of polymer in a good solvent (2-fluorotoluene). Fickian diffusion was observed up to confinements as high as $\lambda_H = R_H/R_P = 1.4$, where R_H and R_P are the polymer and pore radius, respectively. The macroscopic diffusion coefficient D in the porous medium (measured on length scales large compared to R_P) is found to decrease monotonically with increasing molecular weight and λ_H. At $\lambda_H < 0.3$, the diffusion coefficients are in good agreement with those predicted by the hydrodynamic theory for the hindered diffusion of a flexible macromolecule in cylindrical pores. At $0.2 < \lambda_H < 0.5$, D decreases approximately as M^{-1}, a result which is attributed to the hydrodynamic screening effect of the pore walls. At $\lambda_H > 0.6$, a stronger molecular weight dependence emerges, which is inconsistent with the "elongated cigar" model. At large values of λ_H, irregularities in local pore size lead to alterations in polymer conformation and hence changes in entropy as the chain moves. The experimental data agree qualitatively with predictions of the recent entropy barrier theory which is a scaling analysis of the diffusion hindrance based on entropy changes.

Introduction

The diffusion of polymers or other species in porous materials has attracted great interest from different disciplines because of its importance in processes such as chromatography, catalysis, enhanced oil recovery, and membrane separation. The study of hindered polymer diffusion furnishes much insight into topics such as transport in porous media and dynamics of confined polymer chains in gels, pores, and melts.

Polymer molecules diffuse more slowly in porous media than in solution, due to the presence of an obstructing solid phase and hydrodynamic interactions between the polymer and the pore walls. When the size of the macromolecule is comparable to that of the pores, a change in conformation greatly affects diffusion behavior.

Previous studies of diffusion of polymers in porous materials may be divided into two categories: those using systems with well-defined pore geometry such as track-etched membranes[1-6] and those using systems with relatively random pore structures exemplified by porous glasses.[7-14] The central goal of these studies has been to relate the results of phenomenological measurements to the microscopic parameters characterizing the polymer and the porous material. For the diffusion of a flexible polymer across a membrane that can be modeled by a diffusion process in cylindrical pores, the experimental results have been generally consistent with theories of hard sphere diffusion[15-19] and with scaling theories.[20-23] However, a good understanding of polymer diffusion in pores of nonideal geometry has not been attained for several reasons: (1) the pore structure has not been unambiguously characterized; (2) the statics and dynamics of polymers in random pores have not been studied as completely as in pores of idealized geometry; (3) there are discrepancies among the experimental results primarily associated with understanding the movement of diffusant between solution and the porous medium. Systematic and unambiguous measurements of diffusion in porous media are therefore desirable to test further the current models and to stimulate additional theoretical developments.

In our laboratory Bishop and Easwar et al.[12-14] have employed the technique of dynamic light scattering spectroscopy (DLS) for direct measurements of polymer diffusion inside pore space of porous glasses. DLS has significant advantages compared to other techniques as it is insensitive to boundary layer and partition coefficient effects. In this work we extended to new regimes of much higher confinement measurements of the diffusion of linear polystyrene in controlled pore glasses. We have used several dimensional ratios of the polymer and the pores up to a ratio of $\gamma_H = R_H/R_P = 1.4$, where R_H is the hydrodynamic radius of polystyrene in free solution and R_P is the mean pore radius. In interpreting our results, we assume that the macroscopic diffusion coefficient D, measured over distances large compared to the pore radius (i.e. $qR_P \ll 1$ where q is the magnitude of the scattering wavevector), is given by

$$D/D_0 = Xf(\lambda_H) \tag{1}$$

D/D_0 is often referred to as the hindrance factor for diffusion, D_0 is the diffusivity in unbounded solution, and X is the intrinsic conductivity of the porous material.[24,25] The parameter $f(\lambda_H)$ is the size-dependent ratio of diffusivity within the pore space to that in the unbounded solution. For $\lambda_H \to 0$, the factor $f(\lambda_H) \to 1$, thus a measured value of X can be obtained by extrapolating to zero the data of D/D_0 versus λ_H.

When the confinement is relatively weak, the hydrodynamic interactions dominate the diffusion behavior and $f(\lambda_H)$ is equal to the inverse enhanced drag, which is the ratio of the friction coefficient in free solution to that inside the pores. The enhanced drag has been quantitatively predicted in terms of a hydrodynamic theory for hindered diffusion of flexible macromolecules developed by Davidson et al.[2,15] These authors modeled a flexible macromolecule as a porous body, whose average shape and solvent permeability were affected by confinement in a pore. Since the hydrodynamic behavior of the poly-

† Department of Polymer Science and Engineering.
‡ Department of Physics and Astronomy.

0024-9297/90/2223-2022$02.50/0

mer is mainly determined by λ_H and the effect of the permeability is relatively weak, $f(\lambda_H)$ could be approximated by the relation[2,15]

$$f(\lambda_H) \approx 1 - 2.848\lambda_H + 3.269\lambda_H^2 - 1.361\lambda_H^3 \quad (2)$$

for $\lambda_H < 0.8$.

In the present work the dynamic behavior at large λ_H was studied in light of the recently developed theory for the entropy barrier by Muthukumar et al.[26] They modeled the pore structure using an assembly of cavities of dimension L, connected to one another by bottlenecks or gates with cross sectional and longitudinal dimensions C and d, respectively. A polymer chain with a degree of polymerization N translates inside pores thus defined with a diffusion coefficient D, where

$$D = Xd_0 \exp(-\Delta F/k_B T) \quad (3)$$

where ΔF is the conformational free energy difference and D_0 is the diffusivity in free solution; X, as a modification to the original theory, is used in this case to normalize the diffusivity of a chian within a pore space to the macroscopic diffusion coefficient. The fraction of monomer units in the bottleneck, β (noted as f in ref 26), was given by

$$\beta = 1 \qquad dC^2 \gg V_p \quad (4)$$

$$\beta = QN^{-1}C^{(1/\nu)-1} \qquad dC^2 \leq V_p$$

where Q (not used in ref 26) is a constant determined by d, monomer unit length, etc., ν is the exponent relating molecular weight to the polymer size ($R \sim N^\nu$), and V_p is the volume occupied by the polymer. As N increases, β asymptotically approaches $QN^{-1}C^{(1/\nu)-1}$. By calculating ΔF using appropriate weight factors, Muthukumar et al. finally obtained

$$D/XD_0 = \exp\{-N[\beta C^{-1/\nu} + (z^{-1}(1-\beta) - 1)L^{-1/\nu}]\} \quad (5)$$

where z is the average number of cavities which contain $(1-\beta)N$ unconfined segments per gate. It will be shown that there is qualitative agreement between our experimental data and this theoretical prediction.

Experimental Section

Sample Preparation. Linear anionic polystyrenes, each with narrow molecular weight distribution ($M_w/M_n < 1.06$), were used as received. Table I lists the characteristics and sources of the polystryene samples. The peak molecular weight, M_p, obtained from size exclusion chromatography, is used to describe the polystyrene molecular weight noted herein as M. The mutual diffusion coefficient, D_0, in unbounded 2-fluorotoluene solution is measured by DLS at concentrations $C \approx C^*/8$ where C^* is the overlap concentration.[22] (At $C^*/8$, D_0 is greater than that at $C \to 0$ by about 5% at the low molecular weights used in this study and about 10% at the high molecular weights.) For polystyrene with MW $> 3 \times 10^4$ a power law was obtained:

$$D_0\,(37.8\ ^\circ\text{C}, 0.55\ \text{cP}) = 4.63 \times 10^{-4} M_p^{-0.587}\ (\text{cm}^2/\text{s}) \quad (6)$$

The value of the scaling exponent (0.587 ± 0.005) indicates that 2-fluorotoluene is a thermodynamically good solvent, chosen to minimize interchain entanglement and to enable comparison of our results with most existing theories. The hydrodynamic radius was calculated from the Stokes–Einstein equation:

$$R_H = k_B T/6\pi\eta D_0 \quad (7)$$

Polystyrene was dissolved in 2-fluorotoluene (Aldrich, 99+% pure), which was filtered through a 0.2-μm pore diameter teflon membrane (Millipore) before use. The concentration of each solution was normalized to $C^*/8$, where C^* was estimated from M_p as $C^* = [\eta]^{-1}$.

Table I
Characteristics of Polystyrene Samples

code	source[a]	$M_p \times 10^{-3}$ [b]	$D_0 \times 10^7$,[c] cm^2/s	R_H,[d] Å
P7	PC	7	20.0	10.7
P13	PC	13	15.0	27.7
P17	PC	17	13.4	30.9
P24	PC	24	11.5	36.0
P35	PC	35	10.3	40.2
P47	PC	47	8.15	50.8
P50	PC	50	7.88	52.6
P68	PL	68	6.74	61.4
P89	PC	89	5.73	72.3
P100	PC	100	5.43	76.3
P127	PL	127	4.61	89.8
P170	PC	170	3.93	105
P198	PC	198	3.58	116
P350	PC	350	2.50	166
P575	PC	575	2.02	205
P949	PC	949	1.55	267
P1030	PL	1030	1.48	280
P1400	PL	1400	1.26	329
P2050	PL	2050	1.07	387

[a] Abbreviations: PC, Pressure Chemical Co.; PL, Polymer Laboratories. [b] M_p: peak molecular weight by size exclusion chromatography. [c] D_0: diffusion coefficient measured in free solution at concentration $C^*/8$ at 37.8 °C. [d] R_H: hydrodynamic radius calculated from D_0 by using eq 7.

Table II
Characteristics of the Porous Glass Samples[a]

	G75	G275
R_p, pore radius,[b] Å	75	275
v, pore volume,[c] cm^3/g	1.0	1.3
s, surface area,[d] m^2/g	276	105

[a] All data supplied by the manufacturer. [b] Nominal radius from mercury porosimetry. [c] Measured by mercury porosimetry.[29] [d] Measured by BET nitrogen adsorption.[30]

Two controlled pore silica glass samples (Shell Development Co.) were made originally for catalysis purposes by a multistep process starting from silica gels.[27,28] Relevant data from the supplier are shown in Table II. The nominal radii of the pores were measured by mercury porosimetry, and the surface area by BET nitrogen absorption. The porous glasses were amorphous. The local pore structure over small dimensions was believed to be approximately cylindrical in shape, highly branched and highly connected.[28] To prevent adsorption of the polymer, glass surfaces were silanized by reaction of surface activated and thoroughly dried porous glasses with a large excess of chlorotrimethylsilane in toluene solution.

A silanized glass bead (typically 1–2-mm diameter) was mounted inside a dust-free sample cell (10 × 75 mm test tube), and the polystyrene solution was added to the cell containing the glass bead through a 0.5-μm pore diameter membrane filter (Millipore, Milex SR). Sufficient time was allowed for the diffusion coefficient to become stable, typically several days. We note that measured diffusion coefficients have remained stable for over 1 year. The glass and the solution had very similar refractive indices to minimize multiple scattering.

By using controlled pore glasses with small pore radii, we were able to perform light scattering measurements at very high λ_H, which had previously been unattainable.[12] The quantity qR_G was still in a regime suitble for measuring the translational diffusion coefficient of macroscopic diffusion, where R_G is the radius of gyration of the macromolecule in free solution. At $\lambda_H > 1$, the scattering from within the glass fragment still gave a well-defined autocorrelation function (ACF) indicating a finite polymer concentration inside the pores. This is somewhat surprising in view of the existing theories[31,32] and a recent Monte Carlo simulation[33] which indicate that equilibrium partitioning coefficients are expected to become negligible as λ_H approaches 1. Apparently polymer chains can enter the pores to a reasonable extent notwithstanding their deformation by the pore walls.

Dynamic light scattering measurements were made by using a 50-mW Spectra-Physics Model 125 He–Ne laser as the light source. The cell holder assembly was constructed with seven windows at scattering angles ranging from 15° to 155° with axes tilted 5° from the horizontal to diminish stray light. The photon-count autocorrelation function was measured at each of these seven angles with a Langley-Ford Model 1096 digital correlator (Coulter Electronics) which had 256 continguous channels plus 16 channels delayed by 1024 × sample time for measuring the ACF base line.

The diffusion coefficients of the polystyrene fractions in unbounded solution were normally obtained by using a homodyne arrangement while diffusion within a porous glass bead was monitored by using the heterodyne method. The light scattered by the macromolecules was mixed with light statically scattered by the glass matrix which served as a strong local oscillator with an intensity about 50 times that of polymer scattering.

Data Analysis. For the heterodyne arrangement the measured photon-count ACF $G^{(2)}(\mathbf{q},t)$ is related to the normalized scattered electric field ACF $g^{(1)}(\mathbf{q},t)$ by[34,35]

$$G^{(2)}(\mathbf{q},t) = B\{1 + f_c|g^{(1)}(\mathbf{q},t)|\} \quad (8)$$

where $\mathbf{q}$ is the scattering wavevector, t is the delay time, B is the base-line value, and f_c is the heterodyne coherence factor. A least-squares fit of log $G^{(2)}(t)$ to a second-order cumulant expansion[36] was applied where

$$\log\{[G^{(2)}(j\Delta t) - B]/[G^{(2)}(k\Delta t) - B]\} = a + b(j\Delta t) + c(j\Delta t)^2 \quad (9)$$

with k the first data channel used in the fit, Δt the sample time for each channel, and j the channel number. The coherence factor f_c, the average ACF decay rate $\langle\Gamma\rangle$, and the variance of the decay rate distribution μ_2 were derived from the fitting parameters a, b, and c, respectively. For translational diffusion of noninteracting particles over distances large compared to the pore size, $\langle\Gamma\rangle$ is proportional to q^2. The slope of $\langle\Gamma\rangle$ versus q^2 defined the macroscopic diffusion coefficient D of polystyrene in pores. The condition $qR_p \ll 1$ was satisfied for all measurements. The wavelength $(2\pi/q)$ of the fluctuations whose relaxations were monitored by DLS was thus much larger than the pore size.

A correct determination of the ACF base line was essential to the data extraction, especially for heterodyne measurements for which the entire decaying signal amplitude was about 2% of the base-line height, i.e. $G^{(2)}(t = 0) \approx 1.02$ B. Therefore, even an error of 0.2% in the base line would have been unacceptable. A given ACF was judged to be acceptable only when there existed good agreement between the flat region of the decaying curve and the delayed channel base line. The base line $B = G^{(2)}(t \to \infty)$ was used satisfactorily for low and medium λ_H measurements. For high λ_H measurements, for which a sample time of the order of 100 μs had to be used, an acceptable base line was difficult to acquire probably because of factors such as laser intensity variation, relative movements of beam, and sample, etc. This problem was addressed by performing the second cumulants fit with an adjustable base line to minimize the sum of the squared residuals. If the difference in the measured diffusion coefficient using the last channel base line and the adjustable base line was greater than 10%, that run was rejected. A regularized inverse Laplace transform of log $G^{(2)}(t)$ was also performed by using Provencher's CONTIN program[37] to calculate the ACF decay rate distribution and thus the diffusion coefficient distribution. The diffusion coefficients obtained from CONTIN were usually within 5% of those from the second cumulants fit.

Results and Discussion

The translation of polystyrene chains within porous glasses was studied on a time scale, the time for autocorrelation function evolution, at which polymer chains move distances of 5 to 10 times the pore radius, thus averaging over the details of specific pores while revealing the general features of the process. The Fickian diffusion law in which displacement is proportional to $t^{1/2}$ was

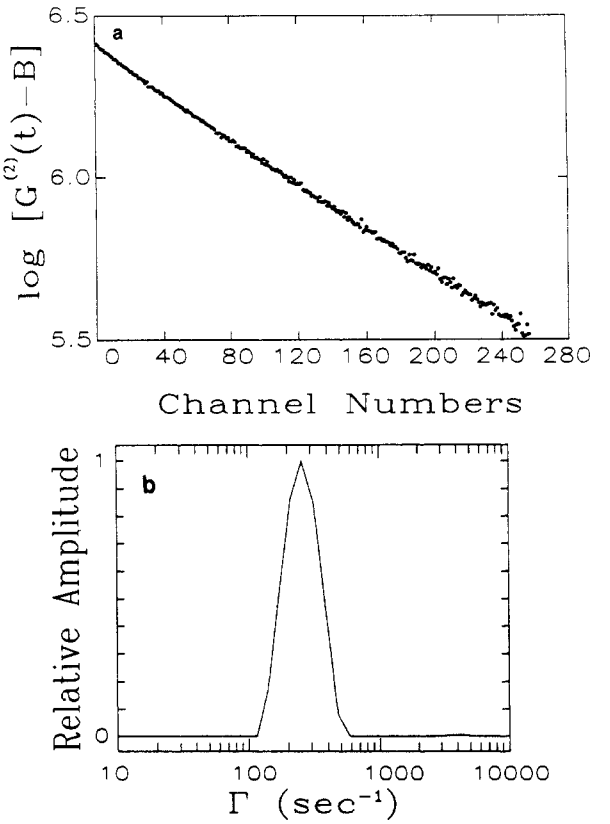

Figure 1. The autocorrelation function (ACF) and its inverse Laplace transform for polystyrene P100 in glass G75 ($\lambda_H = 1.01$) measured at a scattering angle of 35°. (a) Semilogarimic plot of the ACF versus time. Each channel corresponds to a 30-μs sample time. The last channel base line (delayed by 1024 channels) was used. (b) Autocorrelation decay rate spectrum based on scattered intensity obtained from CONTIN[37] program. The macroscopic diffusion coefficient for this system is 3.6×10^{-8} cm^2/s.

observed even for very strongly confined polystyrene chains with $\lambda_H > 1$ in both glasses. This was shown by the linear relation of log $G^{(2)}(t)$ versus t as exemplified by Figure 1a. The ACF decay rate spectrum, based on the scattered intensity, is shown in Figure 1b. The second moment μ_2 (obtained from a least-squares fit to eq 9) normalized to $\langle\Gamma\rangle^2$ provides information about the polydispersity of the diffusion rate:

$$V \equiv \mu_2/\langle\Gamma\rangle^2 \quad (10)$$

For diffusion in free solution $V \approx 0.02$ corresponding to the slight polydispersity of the polymer molecular weights. For the diffusion in the porous glasses, typically $V \approx 0.1$ for the porous glasses G75 at all λ_H values and G275 at $\lambda_H < 0.5$; $V \approx 0.2$ for G275 at $\lambda_H > 0.5$. Considering the nonuniformity of the pores and the small but still significant molecular weight polydispersity that tends to broaden the diffusion rate distribution more strongly than in free solution because of the increasing molecular weight dependence,[38] it seemed justified to treat diffusion within the pores in terms of a single-mode process and therefore to use second cumulant fitting as the main data analysis method.

The hindrance factor D/D_0 versus the size ratio λ_H for the polymer in the glass G275 is shown in Figure 2; D/D_0 decreases monotonically with λ_H as expected. The intrinsic conductivity[24,25] of the porous glass G275 was obtained by extrapolating the data points to $\lambda_H = 0$. It was found that $X = 0.89$, in agreement with what one would expect for this type of glass. The broken line in

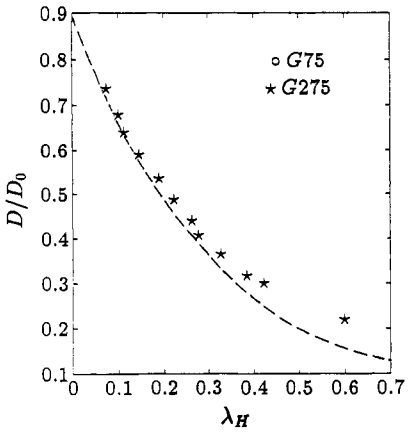

Figure 2. Hindrance factor for macroscopic diffusion (D/D_0) versus polymer to pore size ratio, λ_H. These data are compared to the hydrodynamic theory of flexible polymers in cylindrical pores. The broken line represents the function $D/D_0 = Xf(\lambda_H)$, with $X = 0.89$ and $f(\lambda_H)$ from eq 2, the theoretical prediction of Davidson et al.[2] Only the lower part of the λ_H range studied is shown here.

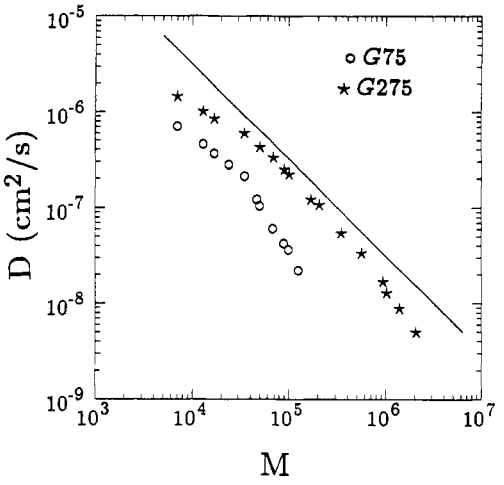

Figure 3. Molecular weight dependence of the macroscopic diffusion coefficients of polystyrene fractions ($7 \times 10^3 < M < 2.05 \times 10^6$) within the porous glasses G75 (O) and G275 (*). The straight line has a slope of −1, which represents the Rouse molecular weight dependence.

Figure 2 represents the function obtained by combining eq 1 and Davidson's prediction,[2,15] eq 2. The experimental data were in good agreement with the hydrodynamic theory up to $\lambda_H \approx 0.3$. This is noteworthy in several respects. First, no adjustable fitting parameter was necessary. Second, eq 2, for the hydrodynamic effect, was directly tested. In Davidson's study, the product of ΦK^{-1} was measured and compared to the theory, it being noted that the partition coefficient Φ itself is often complicated by other factors such as interaction between the poymer and the pore wall.[2] Although eq 2 is expected to be valid up to $\lambda_H \approx 0.8$, agreement with the data clearly deteriorates for $\lambda_H > 0.3$.

The molecular weight dependence of diffusion is shown in Figure 3. When λ_H is close to zero, the hydrodynamic interaction between the polymer and the pore wall vanishes, so that the diffusion behavior in free solution given by $D \propto M^{-\nu}$ is retained as was demonstrated previously.[12,13] Within the range, $0.2 < \lambda_H < 0.5$, the slope is nearly equal to −1 for both glasses thus resembling Rouse behavior.[22,39,40] The Oseen tensor[39] that describes the flow perturbation and the hydrodynamic interaction must vanish at the pore wall, and long-range monomer–monomer interactions (which result in an excluded-volume effect in free solution) are, for the most part, screened by the pore walls. Though this regime is not wide enough to exhibit distinct Rouse molecular weight dependence, the straight line of slope −1 in Figure 3 is intended to show the trend of the data in the intermediate λ_H region. The diffusion behavior in the entire λ_H range should rather be viewed as a continuously evolving process influenced by several factors each manifesting itself to a different extent depending on the degree of confinement.

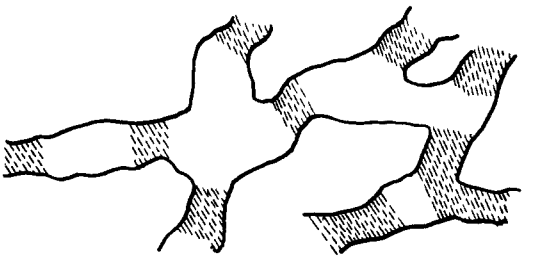

Figure 4. A schematic representation of the pore structure. The shaded areas represent the narrowed passages that play an important role in determining the dynamic behavior of the polymer at large λ_H.

The scaling theories of de Gennes et al.[20-23] that explained membrane transport phenomena successfully were examined for their applicability to polymer diffusion in nonideal pores. By modeling a flexible polymer chain trapped in a cylindrical pore as an elongated cigar with elementary units of the same size as the pore diameter, de Gennes et al. made the scaling prediction

$$D/D_0 \sim \lambda_H^{-2/3} \tag{11}$$

which is equivalent to $D \sim M^{-1}$ for good solvents ($D \sim D_0\lambda^{-2/3} \sim M^{-1}$), so Figure 3 also serves as a comparison of the experimental results to this scaling theory. It can be seen that the molecular weight dependence M^{-1} does not persist through high confinements; instead deviation occurs at a molecular weight corresponding to $\lambda_H \approx 0.6$. Obviously, our results do not support the application of the "elongated cigar" model to pores with nonideal geometry at very high confinements.

When $\lambda_H > 0.6$, D (or D/D_0) decreases with increasing M (or λ_H) more quickly than $D \propto M^{-1}$ (or equivalently $D/D_0 \propto \lambda_H^{-2/3}$). From the empirical relation between the radius of gyration and the hydrodynamic radius of polystyrene;[41] $R_G \approx 1.45R_H$, $\lambda_H \approx 0.6$ is equivalent to $\lambda_G = R_G/R_P \approx 0.9$. Therefore, the begining of the stronger molecular weight dependence is related to the situation in which the dimension of the polymer is approximately the same as the cross sectional pore size. When the polymer equivalent diameter is larger, its conformation must adjust to suit the local pore structure as it moves within the pore space. The sections of the pores in which the entropy of the polymer chain must decrease, e.g. narrow necks, strongly hinder chain motion. This is a major cause of the stronger dependence of D on molecular weight in the regime $\lambda_H > 0.6$ for the porous glasses; for uniformly cylindrical pores, there is no entropy change requirement.

Figure 4 is a possible schematic of the structure of the controlled pore glasses used in these experiments. The important features that are incorporated in the diagram are the following: (1) the pores are highly connected; (2) microscopic nonuniformity of the local pore dimension exists as a result of the manufacturing process; (3) the smallest openings in the pore space (shaded areas) are quite uniform in size. It is known[29,30] that the pore size distribution obtained from mercury intrusion porosimetry reflects the radii of the *restricted* passages, through

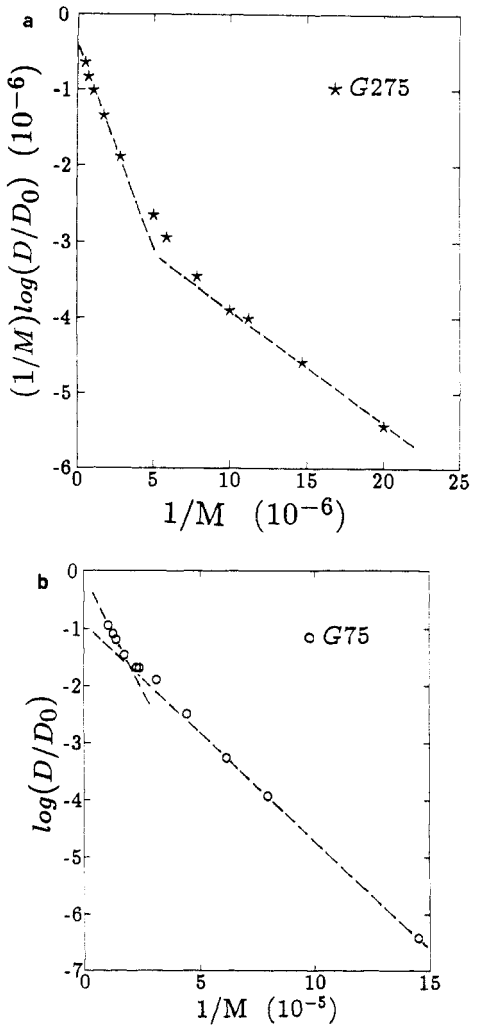

Figure 5. A comparison of the experimental data to the predictions of the entropy barrier theory:[26] (a) glass G275; (b) glass G75. The broken lines are tangent to the data points at the two extremes of the molecular weight range studied.

which all volume is accessible.[29,30] Thus the narrower distribution of R_P measured by mercury intrusion in our samples suggests a relatively uniform size of minimum passage opening. The scanning electron micrographs in ref 12 support this view. In comparing Figure 4 with the "cavity and bottleneck" model we can see that the scaling model for the entropy barrier[26] is appropriate in describing the conformational change accompanying diffusion of strongly confined polymer chains in pores; the parameter C is identified with R_P.

Figure 5 shows a plot of $1/M \log (D/D_0)$ versus $1/M$ as suggested by eq 5 which reduces to

$$N^{-1} \ln (D/D_0) = N^{-1} \ln X - (C^{-1/\nu} - L^{-1/\nu}) \quad \text{if} \quad \beta = 1 \quad (12)$$

or

$$N^{-1} \ln (D/D_0) = N^{-1}(\ln X - Q/C) + [(1-\beta)z^{-1} - 1]L^{-1/\nu} \quad \text{if} \quad \beta = QN^{-1}C^{(1/\nu)-1} \quad (13)$$

A tangent of more negative slope at the larger M (or N) regime is consistent with the predictions of eqs 12 and 13. A transition is thus implied, from a $\beta = 1$ regime at small N in which an entire chain may be accommodated in a bottleneck, to a $\beta < 1$ regime at large N in which only a fraction of the polymer chain can be contained. The transition in Figure 5 and the deviations from $D \propto M^{-1}$ in Figure 3, or equivalently from $D/D_0 \propto \lambda_H^{-2/3}$, occur at similar molecular weights, therefore supporting the assumption that the stronger molecular weight dependence is due to the entropy barrier. Furthermore, the difference in slope between the extremes in the two regimes for G75 is larger than that for G275. The ratio of the differences in slope is comparable to the inverse ratio of the pore sizes, suggesting that the term Q/C may indeed account for the observed transition.

The semiquantitative agreement between the experimental data and the entropy barrier model indicates the importance or even the dominance of the entropy change on the dynamics of highly confined polymer chains in pores with nonuniform geometry. Since R_P measures the dimensions of narrow passages whose counterparts in the model are bottlenecks, λ_H does reflect the determining confinement at larger ratios of polymer to pore sizes. Consequently a low λ_H polydispersity (assured by a low polydispersity in R_P and molecular weight) ensures a low dispersion of the diffusion coefficients as observed in Figure 1.

We note that Muthukumar's scaling analysis for the entropy barrier,[26] from which eqs 5, 12, and 13 were drawn, was based on a model of cavities connected by short bottlenecks. Realistically it is the variation in local pore size that gives rise to the entropy barrier. Useful information can be obtained from nuclear magnetic relaxation analysis[42] that allows characterization of the true distribution in pore sizes.

Conclusions

Diffusion of polystyrene chains within controlled pore silica glasses was studied directly by DLS, under the conditions qR_P and $qR_H \gg 1$. The Fickian diffusion law was observed in all polystyrene fractions in the porous media up to very high confinements. Macroscopic diffusion coefficients were measured and the dependence of these diffusion coefficients on molecular weight and polymer-to-pore size ratio was investigated in terms of the dynamics of confined polymer chains. At small λ_H, hydrodynamic interaction dominated the diffusion behavior. Our results are in good agreement with the predictions based on the hydrodynamic behavior of flexible chains. In the intermediate range, $0.2 < \lambda_H < 0.5$, the diffusion coefficient tends to be inversely proportional to molecular weight, a result stemming from the screening effect of the pore walls. The de Gennes "elongated cigar" model predicts that $D/D_0 \propto \lambda_H^{-2/3}$, equivalent to $D \propto M^{-1}$, for a good solvent in very high confinement regimes ($\lambda_H > 2$). At $\lambda_H > 0.6$, we observe a molecular weight dependence stronger than M^{-1} which is attributed to hindrance due to entropy changes, making the "elongated cigar" model inapplicable for high confinement situations, at least in pores of variable cross section. We suggest that the variation in local pore size imposes restrictions on polymer conformations and thus requires conformational entropy adjustments for polymer movement, which greatly hinders diffusion. Our experimental data are consistent with a scaling model of these entropy barriers.[26]

Acknowledgment. This work was supported in part by AFOSR Grant 88-011. We are grateful to Professors M. Muthukumar, D. Johnson, R. Guyer, and N. Easwar for many stimulating discussions. We thank Drs. S. O'Donahue and K. Eum for many helpful suggestions. The porous glass beads were a gift from Shell Development Co., Houston, TX.

References and Notes

(1) Guillot, G.; Leger, L.; Rondelez, F. *Macromolecules* **1985**, *18*, 2531.
(2) Davidson, M. G.; Deen, W. M. *Macromoleucles* **1988**, *21*, 3474.
(3) Deen, W. M.; Bohrer, M. P.; Epstein, N. B. *AIChE J.* **1987**, *33*, 1409.
(4) Bohrer, M. P.; Patterson, G. D.; Carroll, P. J. *Macromolecules* **1984**, *17*, 1170.
(5) Bohrer, M. P.; Fetters, L. J.; Grizzuti, N.; Pearson, D. S.; Tirrell, M. V. *Macromolecules* **1987**, *20*, 1827.
(6) Guillot, G. *Macromolecules* **1987**, *20*, 2600, 2606.
(7) Johnson, D. L.; Guyer, R. A. Submitted for publication.
(8) Colton, C. K.; Satterfield, C. N.; Lai, C.-J. *AIChE J.* **1975**, *21*, 289.
(9) Tennikov, M. B.; Belen'kii, B. G.; Nesterov, V. V.; Anan'eva, T. D. *Colloid J. USSR (Engl. Transl.)* **1979**, *41*, 526.
(10) Giddings, J. C.; Bowman, L. M., Jr.; Meyers, M. N. *Macromolecules* **1977**, *10*, 443.
(11) Klein, J.; Gruneberg, M. *Macromolecules* **1981**, *14*, 1411.
(12) Bishop, M. T.; Langley, K. H.; Karasz, F. E. *Macromolecules* **1989**, *22*, 1220.
(13) Bishop, M. T.; Langley K. H.; Karasz, F. E. *Phys. Rev. Lett.* **1986**, *57*, 1741.
(14) Easwar, N.; Langley, K. H.; Karasz, F. E. *Macromolecules* **1989**, *22*, 3492.
(15) Davidson, M. G.; Deen, W. M. *J. Membr. Sci.* **1988**, *35*, 167.
(16) Bean, C. P. In *Membranes: A Series of Advances*; Eisenman, G., Ed.; Marcel Dekker: New York, 1972; Vol. 1, p 1.
(17) Anderson, J. L.; Quinn, J. A. *Biophys. J.* **1974**, *14*, 130.
(18) Brenner, H.; Gaydos, L. J. *J. Colloid Interface Sci.* **1977**, *58*, 312.
(19) Paine, P. L.; Scherr, P. *Biophys. J.* **1975**, *15*, 1087.
(20) Brochard, F. *J. Phys. (Les Ulis, Fr.)* **1977**, *38*, 1285.
(21) Brochard, F.; de Gennes, P. G. *J. Chem. Phys.* **1977**, *67*, 52.
(22) de Gennes, P. G. *Scaling Concepts in Polymer Physics*; Cornell University Press: Ithaca, NY, 1979.
(23) Daoud, M.; de Gennes, P. G. *J. Phys. (Les Ulis, Fr.)* **1977**, *38*, 85.
(24) Dullien, F. A. L. *Porous Media: Fluid Transport and Pore Structure*; Academic: New York, 1979.
(25) Lehner, F. K. *Chem. Eng. Sci.* **1979**, *34*, 821.
(26) Muthukumar, M.; Baumgartner, A. *Macromolecules* **1989**, *222*, 1937, 1941.
(27) (a) Haller, W. *Nature* **1965**, *206*, 693. (b) Haller, W. *J. Chem. Phys.* **1965**, *42*, 686. (c) Haller, W. *Phys. Chem. Glasses* **1968**, *9*, 153.
(28) Shiflett, W. K., Shell Development Co. Personal communication.
(29) A special issue devoted to Mercury Porosimetry. *Powder Technol.* **1981**, *29*.
(30) Adamson, A. W. *Physical Chemistry of Surfaces*, 4th Ed.; Wiley-Interscience: New York, 1982.
(31) Casassa, E. F.; Tagami, Y. *Macromolcules* **1969**, *2*, 14.
(32) Giddings, J. C.; Kucera, E.; Russell, C. P.; Myers, M. N. *J. Phys. Chem.* **1968**, *72*, 4397.
(33) Cifra, P.; Bleha, T.; Romanov, A. *Polymer* **1988**, *29*, 1644.
(34) Chu, B. *Laser Light Scattering*; Academic: New York, 1974.
(35) Berne, B. J.; Pecora, R. *Dynamic Light Scattering: With Applications to Chemistry, Biology and Physics*; Wiley: New York, 1976.
(36) Koppel, D. E. *J. Chem. Phys.* **1972**, *57*, 4814.
(37) Provencher, S. W. *Makromol. Chem.* **1979**, *180*, 201.
(38) Lodge, T. P.; Wheeler, L. M.; Tirrell, M. V. *Polym. Bull.* **1986**, *15*, 35.
(39) Yamakawa, H. *Modern Theory of Polymer Solutions*; Harper & Row: New York, 1971.
(40) Aklonis, J. J.; MacKnight, W. J.; Shen, M. *Introduction to Polymer Viscoelesticity*; Wiley: New York, 1983.
(41) Bantle, S.; Schmidt, M.; Burchard, W. *Macromolecules* **1982**, *15*, 1604.
(42) Halperin, W. P.; D'Orazio, F.; Bhattacharja, S.; Tarczon, J. C. In *Molecular Dynamics in Restricted Geometries*; Klafter, J., Drake, J. M., Eds.; Wiley: New York, 1989; p 311.